euspen's 19th International Conference & Exhibition, Bilbao, ES, June 2019
www.euspen.eu

Ultra-precision diamond shaping of microchannels for microfluidic applications

Nicholas Yew Jin Tan[1], XinQuan Zhang[2], Dennis Wee Keong Neo[2], Kui Liu[2], A Senthil Kumar[1]

[1]*Department of Mechanical Engineering, National University of Singapore, 10 Kent Ridge Crescent, 9 Engineering Drive 1, Block EA, Singapore 117576, Singapore*
[2]*Singapore Institute of Manufacturing Technology, 71 Nanyang Drive, Singapore 638075, Singapore*

Email: ntan9792@gmail.com

Abstract
Direct diamond shaping, a novel fabrication technique for microchannels on microfluidic chips, can be achieved by employing Virtual Rotating Tool Shaping (VRTS) on an ultra-precision lathe machine. This technique compensates for the rotation of the workpiece with synchronized movements of the translational axes, allowing the tool rake face to be constantly kept perpendicular to the cutting direction at every point. Akin to the cutting mechanism and the flexibility of single point diamond turning, VRTS allows intricate channel designs to be easily shaped. This subtractive manufacturing method not only allows for a wider range of materials to be shaped, but also provides the flexibility to control the cross-section geometry of the desired channels through customizing the diamond tool. A microchannel of 30 µm was successfully machined using the algorithm developed in an experimental study conducted in a 5-axis ultra-precision machine using a conventional single crystal diamond tool on a PMMA slide.

Ultra-precision, Micromachining, Diamond, Biomedical

1. Introduction

Microfluidics or lab-on-chip technology have seen extensive applications in various fields of research due to their ability to achieve multiple functions by processing minute amounts of liquid, especially in biological and chemical analyses. This has allowed researchers to simulate bodily functions, understand chemical interactions and even conduct clinical diagnostics for patients using point-of-care disposable chips [1-3].

As applications of microfluidics require more unique channel paths and cross-sectional geometries to manipulate flow, advances in fabrication techniques are required to reliably generate such chips, especially when channels as small as 30 µm are of concern. Fabrication techniques such as stereolithography (SLA) and etching have shown limitations in substrate material and selectivity [4, 5], while laser ablation has demonstrated certain difficulties in realizing the desired cross-sectional channel geometry and surface finishing [6-9]. Micro milling, while versatile, also carries its own set of challenges such as poor surface finishing. This requires further post-processing to achieve the desired product and finishing [10, 11].

The current go-to technique for the fabrication of high-mix low-volume microfluidic chips with very fine resolution is soft lithography. However, it is limited to PDMS as the base material, which properties are inferior to those of other common lab materials such as PMMA and Glass [12, 13]. Similarly, soft lithography is prone to channel collapses due to incomplete curing. This is especially so when fine features are desired. Diamond shaping by Ultra-Precision Machining (UPM) thus has the potential to not only cater for a wider range of materials for future development of microfluidic chips, but also reliably maintain productivity while reducing cost.

Many recent developments in UPM, especially in diamond turning techniques, are spurred by the progress in optics and lens fabrication [14-16]. Strict requirements in the optical industry are met by the superior mirror-like surface finish and geometric accuracy that diamond turning offers. Thus, by riding on the advantages of the diamond inserts, shaping of microchannels can be achieved. This net shape method allows microchannels to be formed on a wider range of materials with good surface finishing, with a reduced production time and a lower overall consumable tooling cost. Diamond turning inserts can also be fabricated with customized geometry based on the cross-section of the channel. Additionally, the quality of the channels can be further enhanced by introducing ultrasonic vibrations, generating improved surface finishing and increasing the range of materials that can be shaped [17].

In this paper, a new approach on the generation of tool path for continuous Virtual Rotating Tool Shaping (VRTS), based on the Guilloche Technique [14, 18], is discussed, followed by experimental verification and analysis.

2. Virtual Rotating Tool Shaping

The concept of synchronizing linear and rotary motions for VRTS to fabricate the channels is presented in the following section *(2.1)*, along with the generation of the tool path algorithm based on geometrical calculations *(2.2)*.

2.1. Basic principle of VRTS

The proposed VRTS technique employs four axes of a 5-axis ultra-precision machine, mainly the *X*- and *Y*- translational axes and the *C*- rotational axis, while the *Z-axis* is used to determine the channel depth. For the set-up used in this paper, the tool is set upon the *B*-stage, with the rake facing upwards (Fig. 1).

In order for the diamond tool to shape a curved channel on the workpiece, the rake face of the tool must be aligned perpendicularly to the cutting direction at every instance along the tool path, tangential to the arc. For this to happen, taking into account that the tool is fixed, the workpiece must not only rotate to align the rake face to the cutting direction, but also compensate translationally, by dy and dx, for the run out due to the rotation, $d\theta$, in order to remain in the desired path (Fig. 2). This creates a virtual rotatory axis of the feature without the need to align the axes of the features and the spindle.

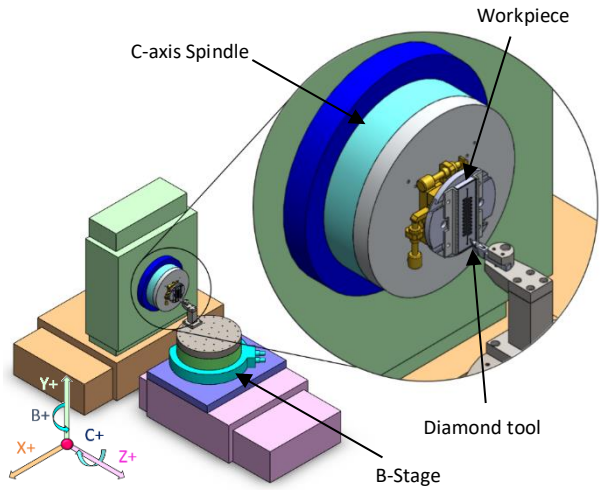

Figure 1. VRTS setup with workpiece on the spindle. The diamond tool was placed on the B-stage, allowing for multiple tools to be set along it for increased productivity.

2.2. VRTS Tool path generation

A simple serpentine design, widely used in microfluidics, was selected as a demonstrator for the algorithm used for VRTS (ref to Fig. 3a for illustration). The algorithm for the tool path generation was developed based on the Cartesian coordinate system (x, y) with the centre of the workpiece as the origin. Considering the Sagitta error tolerance [14], the point cloud developed for the serpentine tool path can be generated with the path starting from the bottom of the chip, as follows:

For **Δy > 0:**

$$y_v \in \begin{cases} [-(2n+1)r + l_v, -(2n+1)r] & \text{, Starting vertical line} \\ [(2n+1)r, (2n+1)r + l_v] & \text{, Ending vertical line} \end{cases} \quad (1)$$

$$x_v = 0 \quad (2)$$

$$y_t = r\sin\theta_t + k_t \quad (3)$$

$$x_t = \sqrt{r^2 - (y_t - k_t)^2} + h_t \quad (4)$$

$$C_t \in \begin{cases} (0, -90] & \text{, Starting arc (CCW)} \\ (-90, 90] & \text{, Right arc (CW)} \\ (90. -90] & \text{, Left arc (CCW)} \\ (-90, 0] & \text{, Ending arc (CW)} \end{cases} \quad (5)$$

$$\theta_t \in \begin{cases} (180, 90] & \text{, Starting arc (CW)} \\ (270, 450] & \text{, Right arc (CCW)} \\ (270. 90] & \text{, Left arc (CW)} \\ (270, 360] & \text{, Ending arc (CCW)} \end{cases} \quad (6)$$

$$y_u = \begin{cases} -2nr & \text{, Starting horizontal line} \\ 2r(2(i-1) - n + 1) & \text{, Horizontal line after right arc} \\ 2r(2i - n) & \text{, Horizontal line after left arc} \\ 2nr & \text{, Ending horizontal line} \end{cases} \quad (7)$$

$$x_u \in \begin{cases} [r, r + l_u] & \text{, Starting horizontal line} \\ [r + l_u, -r - l_u] & \text{, Horizontal line after right arc} \\ [-r - l_u, r + l_u] & \text{, Horizontal line after left arc} \\ [-r - l_u, -r] & \text{, Ending horizontal line} \end{cases} \quad (8)$$

Where x, y and C are the coordinates for the point cloud, denoted by subscripts v, t and u for the vertical, arcing and horizontal lines respectively. Θ represents the included angles and direction of the arc, while h and k signify the x and y coordinates for the centre of the arcs respectively. The total number of loops, n, for this demonstrator is 11, while i symbolizes the loop iteration. The radius, r, used in this demonstrator is 1mm. The vertical runup length l_v is 8.2 mm while the half horizontal length used l_u is 5 mm.

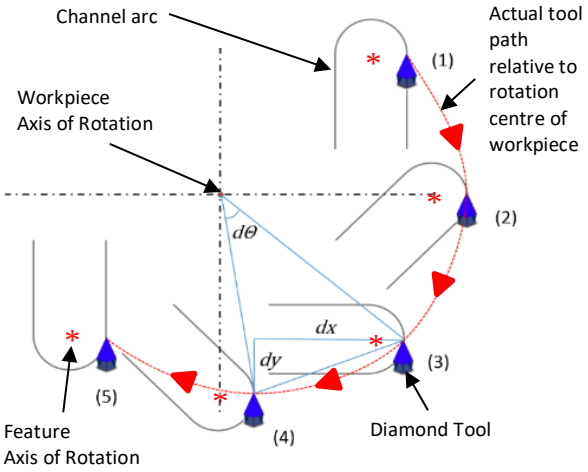

Figure 2. The tool position relative to the spindle centre can be determined by compensating for the linear displacements in the x and y axes. A virtual axis of rotation for the feature can thus be achieved using the workpiece axis of rotation.

A new approach was used for the compensation process which can be applied directly for two-dimensional point clouds. This is done by employing a 2D rigid transformation algorithm along the tool path as follows:

$$\begin{bmatrix} x' \\ y' \end{bmatrix} = \begin{bmatrix} \cos(C) & -\sin(C) \\ \sin(C) & \cos(C) \end{bmatrix} \begin{bmatrix} x \\ y \end{bmatrix} \quad (9)$$

Where x' and y' are the direct compensated coordinate position of the point defined by x and y using the rotation angle of the C stage at the point of interest. Taking the centre of the microfluidic chip as reference, the algorithm is able to directly calculate the entire compensated tool path when applied to the point array generated (Fig. 3b). This only requires the input of the C values rotating in the clockwise or anti-clockwise direction to the next point of interest in order to align the tool along the direction of cut accordingly (Fig. 4).

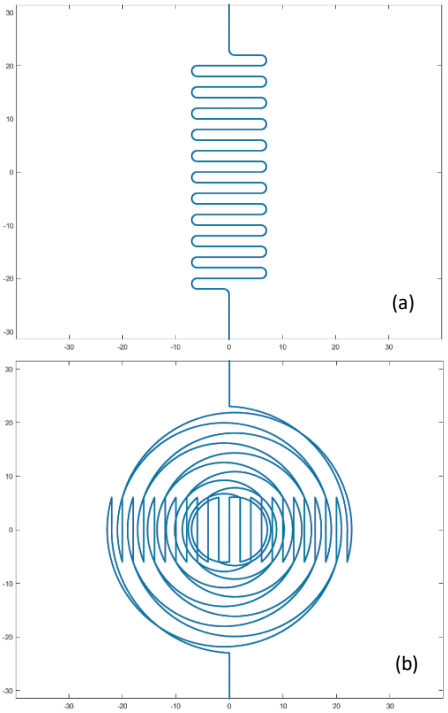

Figure 3. *Point clouds generated using MATLAB (a) Serpentine point cloud with the XY coordinate system. (b) Compensated point cloud which enables VRTS in the XY coordinate system. Taking into account the C-axis, the following tool path will be generated*

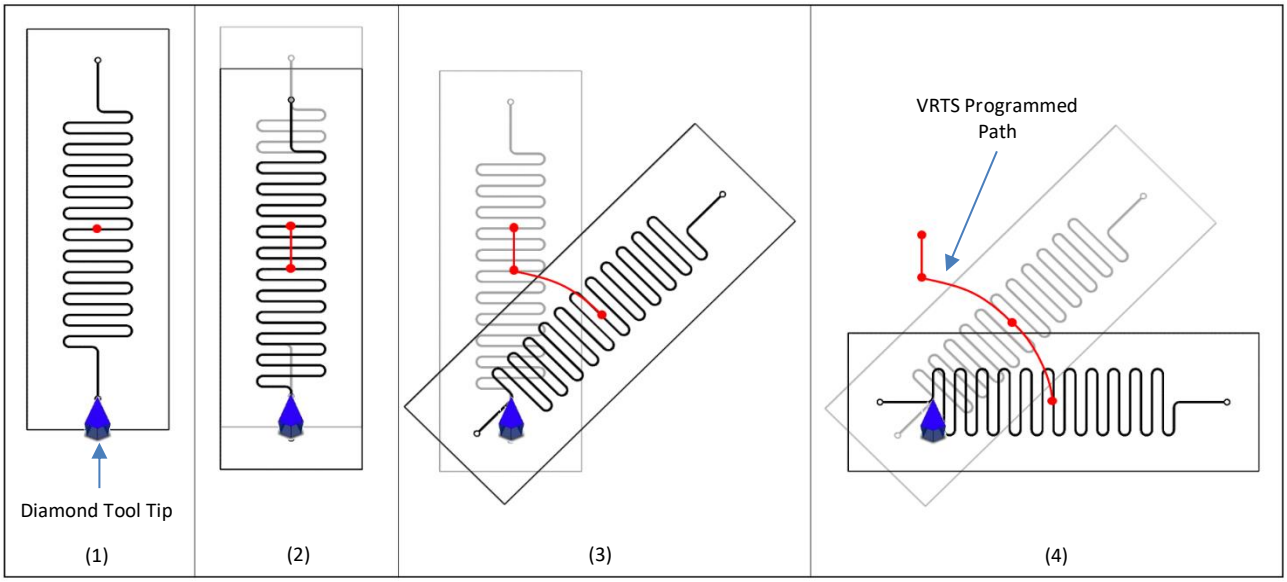

Figure 4. *Simulated motion of the workpiece while VRTS was employed to machine the first turn of the serpentine microchannel. The red dot represents the centre of the C stage, as well as the workpiece axis of rotation. (1) The starting point of the workpiece aligns with the tool and moves to the required depth of cut (2) The workpiece moves down, shaping out a straight channel in the process. (3) The machine initiates the shaping of the first curve using the rotation of the C-axis as well as compensating linearly in order to continue shaping along the desired path, while maintaining the rake face of the tool perpendicular to the tool path. (4) A 90 deg quadrant is fully shaped with a radius of 1 mm, located 23 mm from the centre of rotation.*

3. Experimental verification

To verify the VRTS technique, the process was conducted on a 5-axis ultra-precision machine. The physical setup of the machine is presented in Figure 5. A PMMA slide measuring 75 mm by 25 mm with a thickness of 1mm was used as the substrate workpiece.

A microchannel was created using a conventional single crystal natural diamond tool with a nose radius of 14 µm, 20° included angle, 120° opening angle and a 15° cylindrical front clearance angle for shaping. Due to the tapered geometry of the tool, the channel width can be derived as a function of the depth given as follows, where the depth is greater than the tool nose radius:

$$W = 2\left\{t\sin\left(\frac{\xi}{2}\right) + \left[D - t\left(1 - \cos\left(\frac{\xi}{2}\right)\right)\right]\left[\tan\left(\frac{\xi}{2}\right)\right]\right\} \qquad (10)$$

Where ζ and ξ are the opening and included angles respectively, while t is the tool nose radius. This resulted in a theoretical channel width of 32.36 µm at the depth of 30 µm and a draft angle of 10° on each side of the channel walls (Fig. 6). Equation 10 can typically be applied to estimate the channel width for most conventional diamond tools if the depth of cut is larger than the tool nose radius.

The nature of the setup also allowed a second diamond tool to be positioned beside the shaping tool (Fig. 5). The ability to position multiple tools significantly increases the productivity as multiple sequences can be performed together in a single set up. This greatly reduces the lead time and set up time required to change and re-zero each tool before using. The second tool in this set up was used to face the PMMA slide to ensure the flatness of the chip produced, which is an important requirement for bonding of polymer microfluidic chips to prevent channel collapses.

The point cloud generated had approximately 420,000 points, at 0.003 mm between each point. This gave a machining feed rate of a constant 3mm/s and the total machining time, including the tool entry and exit, amounted to approximately 8 minutes per run. The even spacing between the points ensures that the local walking speed of the tool remains constant regardless of the feature being machined. The process ran consecutively with two rough cuts of 12.5 µm and a 5 µm finishing cut using the same point cloud, amounting to a channel depth of 30 µm.

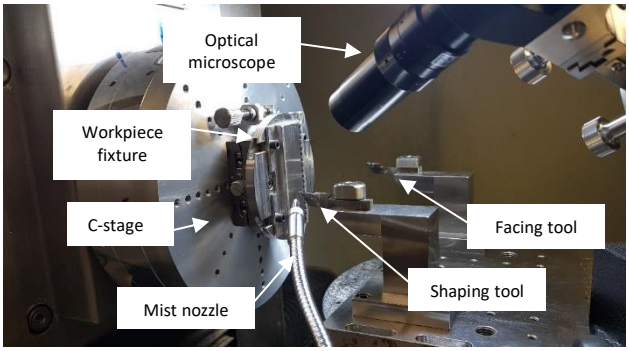

Figure 5. *Physical setup for VRTS on a 5-axis ultraprecision machine. As the tools are set on the B-stage of the machine, multiple tools can be positioned alongside the shaping tool. This allows the machine to perform multiple sequences (facing, change in features, etc.) with a single setup, reducing the lead time and increasing the productivity.*

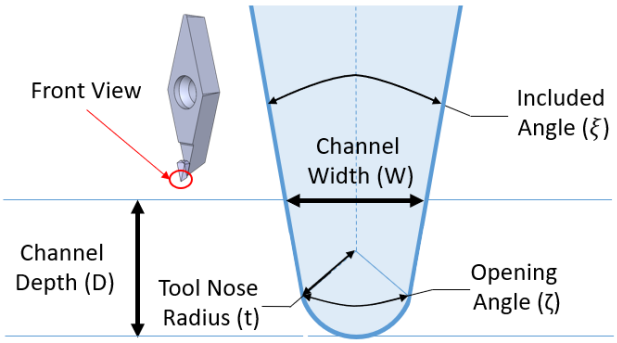

Figure 6. *The rake face of a conventional diamond tool and its notable features. Eqn. 10 can be used to determine the channel width as a function of the respective angles and the depth of cut (if the depth of cut is more than the tool nose radius).*

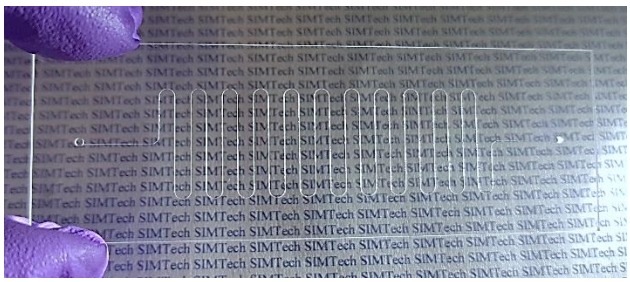

Figure 7. *30 µm Microfluidic Channel successfully machined using VRTS on a 75 mm by 25 mm PMMA slide.*

4. Results and Discussion

Using the VRTS technique, the microchannels were successfully machined with the serpentine design on the surface of the PMMA slide, as shown in Figure 7. A confocal microscope was then used to investigate the quality of the diamond shaping process (Fig. 8).

The surface roughness along the bottom of the channel was measured with an average Ra of 24 nm, which corroborates with the excellent surface finishing that ultraprecision diamond machined products yield. The depth of the channels were measured to have an average depth of 30.297 µm. This minor deviation from the set value of 30 µm can be attributed to the contact method used when determining the surface of the workpiece before the commencement of the machining process.

The channel width of the channel was measured with an average of 32.09 µm. The slight variation from the theoretical width may be due to the perpendicular alignment of the tool to the workpiece or due to the plastic-elastic behaviour of the PMMA substrate.

With the successful shaping of the microchannels, VTRS has shown to be a viable method to produce high quality microchannels for microfluidic applications, with the production reliability of conventional machining processes.

5. Conclusion

Direct diamond shaping via Virtual Rotating Tool Shaping (VRTS) was successfully employed to fabricate microchannels in a serpentine design. The shaping was done by applying a point-by-point rigid rotation algorithm to continuously align the cutting direction of tool vertically to the workpiece. This compensates the linear displacement due to the rotation of the workpiece in synchronization, allowing complex channels to developed. The conventional diamond tool used will define the dimensions and profile geometry of the channel shaped. The surface roughness of the machined channels was also measured, with an average Ra of 24 nm.

This process of creating microchannels thus allows for a wider array of materials to be used as substrates for microfluidic applications besides PDMS. As the channels are shaped using mechanical means of removal, it provides a more reliable method to produce microchannels for microfluidic applications, while also having the flexibility to define the channel profile via the tool geometry.

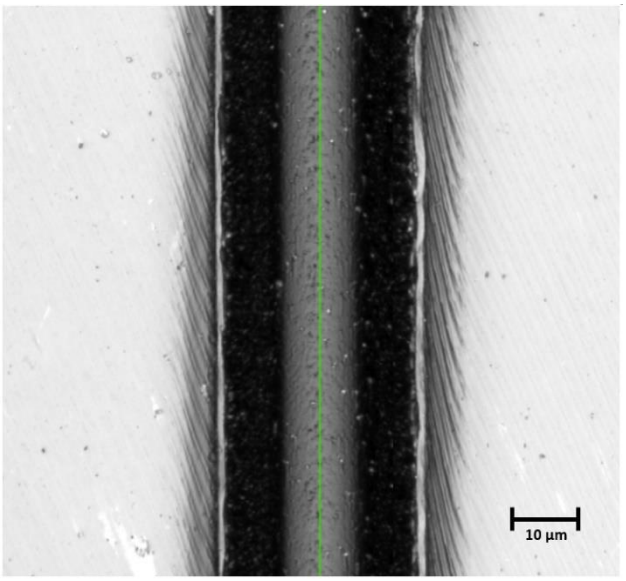

Figure 8. *The surface roughness along the microchannels was measured with an Ra of 0.024 µm using a confocal microscope (along green line).*

References

[1] H Sakamoto, R Hatsuda, K Miyamura, S Sugiyama 2013 *Micro Nano Lett.* ***8***(6274-276

[2] Y Xing, M Nourmohammadzadeh, JE Mendoza Elias, M Chan, Z Chen, JJ Mcgarrigle, J Oberholzer, Y Wang 2016 *Biomed. Microdevices* ***18***(80)

[3] CH Ahn, JW Choi, G Beaucage, J. Nevin, JB Lee, A Puntambekar, and RJY Lee 2004 Proc. IEEE 92(1) 154–73.

[4] CMB Ho, SH Ng, KHH Li, YJ Yoon 2015 *Lab Chip* ***15***(18) 3627-37

[5] B Ziaie, A Baldi, M Lei, Y Gu, RA Siegel 2004 *Adv. Drug Deliv. Rev.* **56**(2) 145-72

[6] R Suriano, A Kuznetsov, SM Eaton, R Kiyan, G Cerullo, R Osellame, BN Chichkov, M Levi, S Turri 2011 *Appl. Surf. Sci.* **257**(14) 6243-50

[7] R McCann, K Bagga, R Groarke, A Stalcup, M Vazquez, D Brabazon 2016 *Appl. Surf. Sci.* **387** 603 – 08

[8] G Li, G. Feng, S Wang, H Zhang, Z Wang, S Zhou 2017 *Optik* **140** 953-58

[9] S Lo Turco, G Nava, R Osellame, KC Vishnubhatla, R Pamponi 2014 *Opt. Mater.* **36**(1) 102-05

[10] KV Christ, BB Smith, FE Pfefferkorn, KT Turner 2010 *ICOMM/4M* ***71*** 423-30

[11] DJ Guckenberger, TE de Groot, AMD Wan, DJ Beebe, EWK Young 2015 *Lab Chip* ***15***(11) 2343-24

[12] MW Toepke and DJ Beebe 2006 *Lab Chip* ***6***(12) 1484-86

[13] KJ Regehr, M Domenech, JT Koepsel, KC Carver, SJ Ellison-Zelski, WL Murphy, LA Schuler, ET Alarid, DJ Beebe 2009 *Lab Chip* ***9***(15) 2132-39

[14] Liu K, Wu H, Liu P, Shaw KC 2011 *Int. J. of Adv. Manuf. Technol.* ***57****(1) 85-99*

[15] Neo DWK, Kumar AS, Rahman M 2015 *Precis. Eng.* ***41*** 55-62

[16] Huang R, Zhang XQ, Rahman M, Kumar AS, Liu K 2015 *CIRP Ann. Manuf. Technol.* ***64*** 121-24

[17] T Moriwaki, E Shamoto 1991 *CIRP Ann. Manuf. Technol.* ***40*** 559-62

[18] S To, ZW Zhu, HT Wang 2016 *CIRP Ann. Manuf. Technol.* ***65*** 475-78